Microchemical Journal 130 (2017) 168–178

Contents lists available at ScienceDirect

Microchemical Journal

journal homepage: www.elsevier.com/locate/microc

Novel glycine-functionalized magnetic nanoparticles entrapped calcium alginate beads for effective removal of lead

Renu Verma [a], Anupama Asthana [a], Ajaya Kumar Singh [a,*], Surendra Prasad [b,*], Md. Abu Bin Hasan Susan [c]

[a] Department of Chemistry, Government V.Y.T. Postgraduate Autonomous College, Durg, Chhattisgarh 491001, India
[b] School of Biological and Chemical Sciences, Faculty of Science, Technology and Environment, The University of the South Pacific, Private Mail Bag, Suva, Fiji
[c] Department of Chemistry, Dhaka University, Dhaka, Bangladesh

ARTICLE INFO

Article history:
Received 16 July 2016
Accepted 14 August 2016
Available online 16 August 2016

Keywords:
Magnetic nanoparticles
Functionalization of nanoparticles
Calcium alginate beads
Pb(II) adsorption
Pb(II) removal

ABSTRACT

The magnetic Fe_3O_4 nanoparticles were functionalized with glycine at pH 6. The glycine functionalized magnetic nanoparticles (GFMNPS) were then entrapped into alginate polymer as beads and used as adsorbent for the removal of Pb(II) ions. The developed adsorbents were characterized by Fourier transform infrared spectroscopy, vibrating sample magnetometer and scanning electron microscopic analysis. The surface of beads contain amino and carboxylate groups which make them effective adsorbents for the removal of Pb(II) ions. The adsorption of Pb(II) ions from aqueous solution was found to be highly pH dependent. 92.8% Pb(II) was removed just in 10 min. The kinetic data fitted well with pseudo second order model and the equilibrium was reached in 100 min with 99.8% removal of Pb(II) ions from aqueous solution. The adsorption isotherm strictly followed Langmuir model with the maximum adsorption capacity of 555.5 mg/g of the adsorbent. The thermodynamic study confirmed that the adsorption was spontaneous and endothermic in nature. The adsorbent could be regenerated four times simply by 0.2 M HNO_3 retaining 90% of the adsorption capacity. The synthesized adsorbent was found to be eco-friendly, cost-effective, efficient and superior over other polymer based adsorbents for removal of Pb(II) ions from aqueous solution.

1. Introduction

Many heavy metals that have been increasingly discharged into the surface water are non-degradable and tend to accumulate along the food chain while many are known to be toxic or carcinogenic [1]. Pb(II), as one of the most toxic heavy metals, exists in the wastewater of many industries, like plating, tanneries, oil refining, mining etc. [1]. Therefore, water pollution has been a major concern around the globe. Rapid industrial development has been increasingly generating huge amounts of effluent comprising of higher concentration of pollutants which inter alia include heavy metal ions. The effluents are released into the environment which contaminates surface water as well as ground water, posing serious threat to communities for drinking water. Majority of the heavy metals serve as slow poisons for human beings and other living bodies and are detrimental to aquatic environment because of their non-biodegradable, carcinogenic and persistent nature [1–3]. Industrial effluents, in most instances, contain higher concentration of lead [4]. Living organisms can accumulate Pb(II) present in the environment. Pb(II) shows significant environmental and health hazards due to its ability to damage nerve system and causes renal kidney disease, mental retardation, nephrite syndrome, cancer, headache, diarrhoea and anemia in human beings [1]. Thus, the control of Pb(II) pollution in wastewater is of significant public interest [1–4]. The Pb(II) containing wastewater in the environment is anthropogenic. Industries like lead-acid batteries, paint, phosphate fertilizer, electronic and petroleum along with forest fires, mining activity, automobile emissions, corrosion of lead containing piping introduce Pb(II) every day into the environment. The maximum permissible limit of lead in drinking water is 0.05 mg/L as recommended by World Health Organization (WHO) [5,6].

With ever increasing demand of safe and clean water in the society, the development of improved technologies for effective removal of toxicants like heavy metal ions from water resource or wastewater has been a challenging task before analytical chemists. The traditional methods such as ion-exchange, chemical oxidation/reduction, chemical precipitation, ultra-filtration, and reverse osmosis, etc. have several disadvantages such as high expense, prolonged period with less efficiency, and production of other waste products [7]. The adsorption method is superior to other techniques because of low-cost, simplicity of design, ease of operation, high effectiveness and the possibility of reuse of the adsorbents. However, recent bias has been shifted to nanotechnology since nanoscale size, large surface area to volume ratio or efficiency,

* Corresponding authors.
E-mail addresses: ajayaksingh_au@yahoo.co.in (A.K. Singh), prasad_su@usp.ac.fj (S. Prasad).

http://dx.doi.org/10.1016/j.microc.2016.08.006
0026-265X/

economic viability and environmental friendliness are all considered useful in the removal of heavy metal ions. The constraints, however, have been issues regarding mass transport and excessive pressure drops in fixed bed column and difficulties in separation and reuse are vulnerable for ecosystem as well as human health with the risk of the release of nanoparticles (NPs) into the environment [6,8]. To overcome the issues, nanocomposites (NCs) coated with solid materials with enhanced mechanical strength has been found to be promising for long term use [8]. Thus, polymeric support is an excellent option for nanoparticles to ensure high mechanical strength, better chemical stability, bio-compatibility and improve hydrophobic/hydrophilic balance through nanoparticle-matrix interaction [8–10]. Alginate, a natural polysaccharide extracted from brown seaweeds, is one of the best choices for the removal of water pollutants as it has inherent advantages like inexpensive, non-toxic, biodegradable and abundant [3,9]. The carboxylate groups present in the polymer structure provide the ability to bind metal ions on their surface and thus leads to the removal of the metal ions from water and wastewater samples [3,9,11]. Thus, the magnetic separation techniques may be innovatively applied to such polymers as a promising means of water purification.

The magnetic sorbents are easily separated by external magnetic field, which helped to utilize iron oxide composite polymers for the removal of organic and inorganic pollutants [6]. The magnetic NPs modified with α-ketoglutaric acid [12] and NCs with chitosan and poly(acrylic acid) have also been used for the removal of Cu(II) ions from aqueous solution [13]. Lanthanum adsorption has also been studied by using iron oxide loaded alginate beads [14]. The magnetic alginate beads have been prepared and used for the adsorptive removal of Co(II), Ni(II) and Pb(II) ions from wastewater sample [3,11,15]. The amino acid, glycine, has been used for functionalization of magnetic NPs due to the fact that it is a short molecule and carboxylate groups are easily adsorbed on the surface of magnetic NPs while amino groups on their surface remains available for interaction of metal ions [16]. Some works with amino functionalized magnetic NPs are evident for effective removal of heavy metals [16,17]. Polymer has been used as adsorbent but entrapping magnetic NPs increases the mechanical and thermal strength of polymer and also provides more functional groups on their surface which enhance adsorption capacity of adsorbent [6,9,11,13,16]. The surface modified magnetic NPs were entrapped into the polymer such as vinyl functionalized magnetic iron-imprinted polymer has been used for the determination as well as removal of Pb(II) ions [18]. The carboxylated cellulose nanofibrils-filled magnetic chitosan hydrogel beads have successfully been used by Zhou and co-workers for the removal of Pb(II) [19]. Pb(II), being one of most toxic heavy metals, has stimulated research on its removal from wastewater and drinking water. Thus there has been continuous considerable emphasis on the development of methods for the removal of Pb(II) [1–6,15,18–22].

The amino functionalized magnetic NPs entrapped polymer beads is an innovative technique for water purification and given the fact that Pb(II) is one of the most widespread water pollutants [1,22], the development of cost-effective and environmental friendly technologies for the removal of Pb(II) ions from water and wastewater samples is of global interest. Thus, in our continued efforts in developing cost-effective analytical techniques for detection of pollutants [22–28] including Pb(II) ions [22] and fluoride removal methods [29–31], we were looking for a cost-effective method for the removal Pb(II) ions from aqueous samples. With the above background, in the present work, novel glycine-functionalized magnetic nanoparticles-entrapped calcium alginate beads (GFMNPECABs) have been synthesized and characterized, and studied as an adsorbent for removal of Pb(II) ions from aqueous solution. The adsorption isotherms, adsorption kinetics and thermodynamic studies have been performed in batch experiments method. The method for the synthesis of the novel adsorbent GFMNPECABs for the removal of Pb(II) ions from aqueous sample and its advantages like simplicity, inexpensiveness, high adsorption capacity and good reproducibility have been highlighted in the present communication.

2. Material and methods

2.1. Materials

Lead nitrate, $Pb(NO_3)_2$, and glycine ($C_2H_5NO_2$) purchased from Merck (Mumbai, India). Sodium alginate $(C_6H_7NaO_6)_n$, ferric chloride hexahydrate ($FeCl_3 \cdot 6H_2O$), ferrous chloride dihydrate ($FeCl_2 \cdot 2H_2O$), HN_4OH and HCl were purchased from Loba Chemie (Mumbai, India). All chemicals used were of analytical reagent grade and used without further purification. All solutions were prepared in triple distilled water.

2.2. Equipment

Fourier transform infrared spectrometer (Frontier FT-IR/NIR, PerkinElmer, USA) was used to record the infrared spectra of glycine functionalized magnetic nanoparticles (GFMNPs) and GFMNPECABs in the range of 400–4000 cm^{-1} using KBr pellets. The surface morphologies of the GFMNPs, powdered GFMNPECABs and GFMNPECABs samples were analyzed by scanning electron microscope (JEOL, JSM-6490LA Analysis Station, USA). The concentration of Pb(II) ions was measured by atomic adsorption spectrophotometer (240FA AA, Agilent Technologies, USA). The vibrating sample magnetometer (model 7410, Lake Shore, Cryotronics, USA) was used to record the magnetization curve of non-functionalized magnetic nanoparticles (MNPs) and GFMNPs.

2.3. Synthesis of magnetic nanoparticles

The NPs were prepared by the co-precipitation method, where Fe(II) and Fe(III) ions were precipitated by ammonia solution under hydrothermal conditions (32). The ferric chloride and the ferrous chloride (mole ratio 2:1) were dissolved in water and 1.5 M NH_4OH solution added drop-wise at 25 °C under continuous stirring while maintaining pH 10. The black precipitate formed was heated at 80 °C for 30 min with continuous stirring. The synthesized Fe_3O_4 NPs were separated by external magnetic field, washed several times with triple distilled water and finally dried in the oven at 250 °C for 2 h [32].

2.4. Modification by glycine

The surface of Fe_3O_4 NPs was modified with glycine, where magnetic NPs (1 g) was treated with 0.5 mol/L glycine solution. The pH of the solution was maintained at 6. The NPs were separated by external magnetic field, and then GFMNPs were washed with triple distilled water and vacuum dried at room temperature [33].

2.5. Preparation of GFMNPECABs

Sodium alginate powder (1.5 g) was dissolved into 50 mL triple distilled water with magnetic stirring for a period of 2 h which gave a homogenous viscous solution. Then, 1 g of glycine modified Fe_3O_4 NPs was mixed under constant stirring. After drop-wise addition of the above mixture of viscous solution into the $CaCl_2$ solution using a syringe, GFMNPECABs were formed. The beads were left in the $CaCl_2$ solution for 24 h to obtain stable gel beads. The beads were washed several times with triple distilled water and stored in distilled water for use as an adsorbent. The beads turned red brown due to entrapment of modified magnetic NPs by the alginate polymer. A schematic representation of synthetic pathway of GFMNPECABs and photograph of gel beads attracted by external magnetic field is presented in Fig. 1.

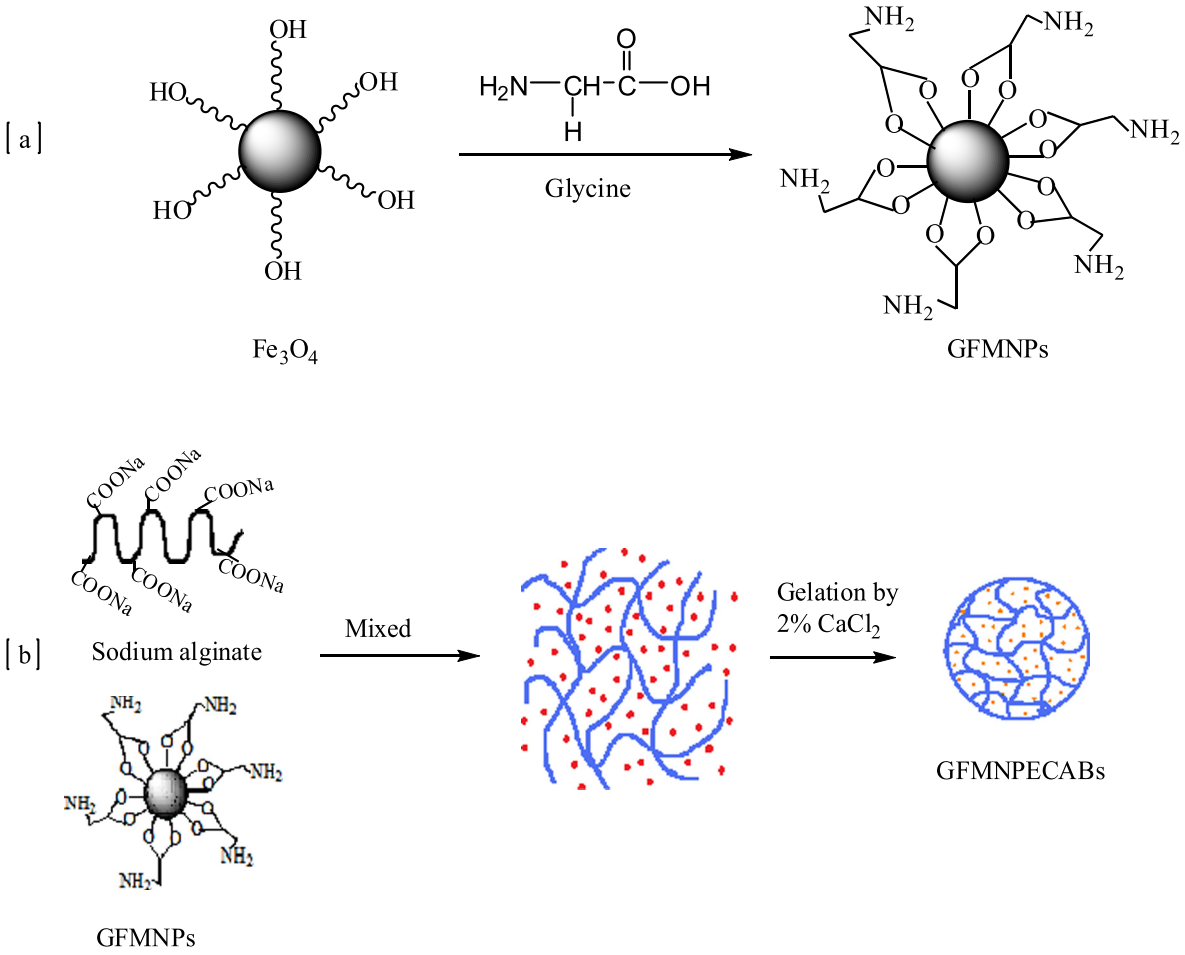

Fig. 1. (a) Schematic representation of possible pathway for preparation of GFMNPs; (b) formation of GFMNPECABs and (c) photograph of GFMNPECABs attracted by a magnet.

2.6. Batch adsorption experiment

The percentage removal of Pb(II) ions by GFMNPECABs was studied by batch adsorption experiment. Pb(II) solution (10 mg/L) was taken into Erlenmeyer flasks with fixed volume (10 mL) to optimize the system variables. Thermostatic shaker bath was used for shaking the mixture while performing thermodynamic studies. The percentage removal (R) of Pb(II) ions was calculated using Eq. (1) where C_o and C_e are the

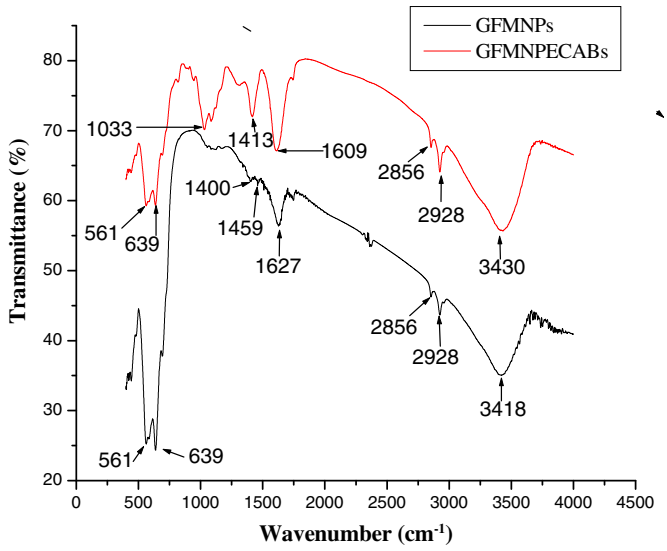

Fig. 2. The FTIR spectra of glycine functionalized magnetic nanoparticles (GFMNPs) and glycine-functionalized magnetic nanoparticles-entrapped calcium alginate beads (GFMNPECABs).

initial and equilibrium concentrations of Pb(II) ions (mg/L), respectively [34].

$$R(\%) = \frac{C_o - C_e}{C_o} \times 100 \quad (1)$$

The equilibrium adsorption isotherms and the effects of the variables like pH and time were studied using aqueous solution of Pb(II) ions at different concentrations and temperatures. 0.1 g of the adsorbent i.e. GFMNPECABs was added to an Erlenmeyer flask containing 10 mL Pb(II) ions solution of different concentrations while the pH was adjusted to 6 using 0.1 M HCl and 0.1 M NH_4OH. The adsorption mixture containing GFMNPECABs was shaken for 2 h, so as to reach equilibrium at different temperatures, for the determination of the maximum adsorption capacity. The adsorption capacity of GFMNPECABs was determined using Eq. (2) where C_o and C_e are the initial and equilibrium concentration of Pb(II) ions (mg/L), respectively, q_e is the equilibrium adsorption capacity (mg/L), m is the mass of the adsorbent (g) and V is the volume of the solution (L).

$$q_e = \frac{(C_o - C_e)V}{m} \quad (2)$$

The kinetics of adsorption GFMNPECABs was studied using 10 mL of 10 mg/L Pb(II) solutions at different temperatures. The solution containing 0.1 g adsorbent at pH 6 was shaken in a thermostatic water bath shaker and the remaining concentration of Pb(II) ions was determined at different time intervals. The kinetic adsorption capacity was calculated using Eq. (3) where q_t is the adsorption capacity at time t while other terms have their usual meaning (vide supra).

$$q_t = \frac{C_o - C_t}{m} \times V \quad (3)$$

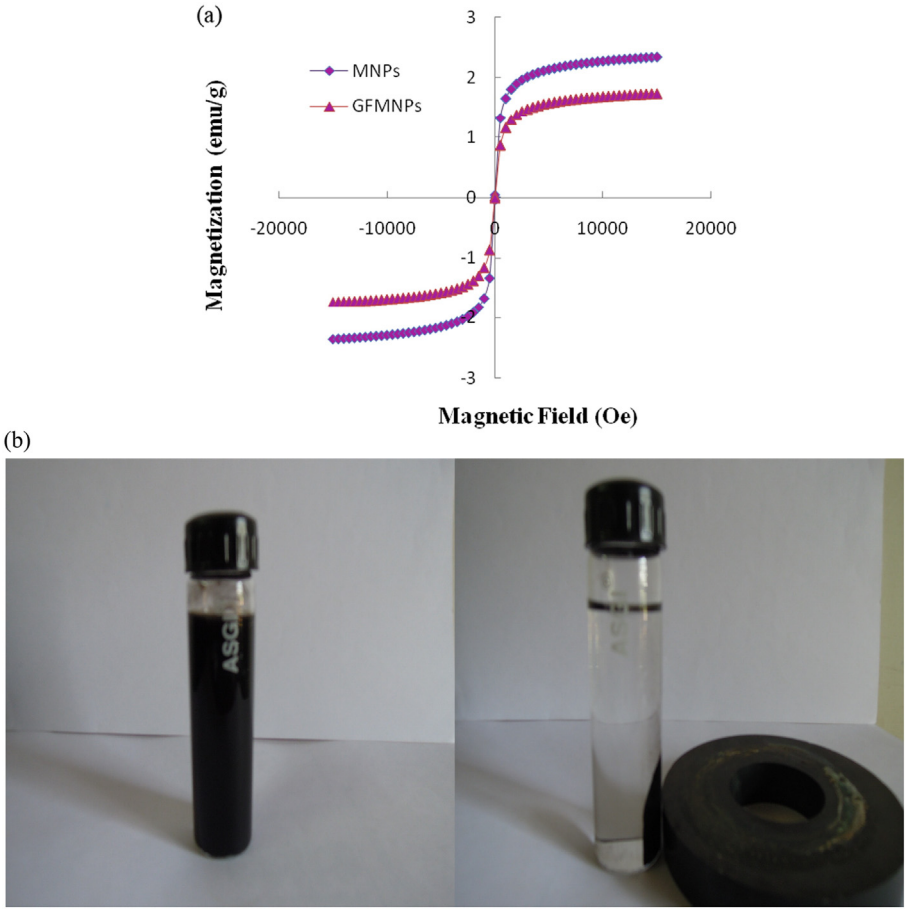

Fig. 3. (a) Magnetization curve of non-functionalized MNPs and GFMNPs, (b) the separation of GFMNPs by external magnetic field just in 5 min.

3. Results and discussion

3.1. Characterization of adsorbent

Fourier transform infrared (FTIR) spectra of GFMNPs and GFMNPECABs with their band assignments are shown in Fig. 2. The bands at 561 cm^{-1} and 639 cm^{-1} are attributed to Fe-O vibration mode and were identified at the same wavenumbers for GFMNPs as well as for GFMNPECABs. The symmetric (V_s) and asymmetric (V_{as}) stretching bands of glycine carboxylate (-COO^-) groups in GFMNPs appeared at 1400 cm^{-1} and 1627 cm^{-1}. The separation of wave number ($\Delta = 227\ cm^{-1}$) for V_s -COO^- and V_{as} -COO^- indicated a bridging bidentate type of interaction which suggested that glycine was chemisorbed on the surface of Fe_3O_4 NPs through carboxylate groups while amine groups remained free [35]. The GFMNPECABs showed sharp bands at 1413 cm^{-1} and 1609 cm^{-1}. The band at 2928 cm^{-1} appeared due to Fermi interaction of the NH_3 group with V_s of -COO^- groups and amine moiety bending mode δ-NH_3 showed that NPs are coated by glycine [33]. The weak band observed at 2856 cm^{-1} was due to V_s of -CH_2 group. The spectra of GFMNPs and GFMNPECABs showed same bands at the same positions; 2928 cm^{-1} and 2856 cm^{-1}. The band at 3418 cm^{-1} is attributed to the -OH stretching in GFMNPs which shifted to 3430 cm^{-1} in the case of GFMNPECABs. The V_s -COO^- and V_{as} -COO^- bands at 1459 cm^{-1} was shifted to 1413 cm^{-1} while 1627 cm^{-1} shifted to 1609 cm^{-1} which confirmed the electrostatic attraction between the -NH_2 and -COO^- groups on the surface of GFMNPs and GFMNPECABs.

The magnetization curves of GFMNPs and the non-functionalized MNPs were recorded using a vibrating sample magnetometer (VSM) at room temperature and are shown in Fig. 3a. The values of saturation magnetization were found as 2.352 and 1.732 emu/g for non-functionalized MNPs and GFMNPs respectively. The decrease in saturation magnetization in the case of the GFMNPs was due to the chemisorption of glycine on the surface of MNPs [33]. The NPs have good magnetic properties and thus were easily separated by external magnetic field. The magnetization data indicated small remanence and coercivity in hysteresis loops. The suspension of GFMNPs was separated by external magnetic field just in 5 min as shown in Fig. 3b where a transparent solution was achieved.

The scanning electron microscopic (SEM) images indicated that the surface of GFMNPs were rough with a large surface area (Fig. 4a,b). The

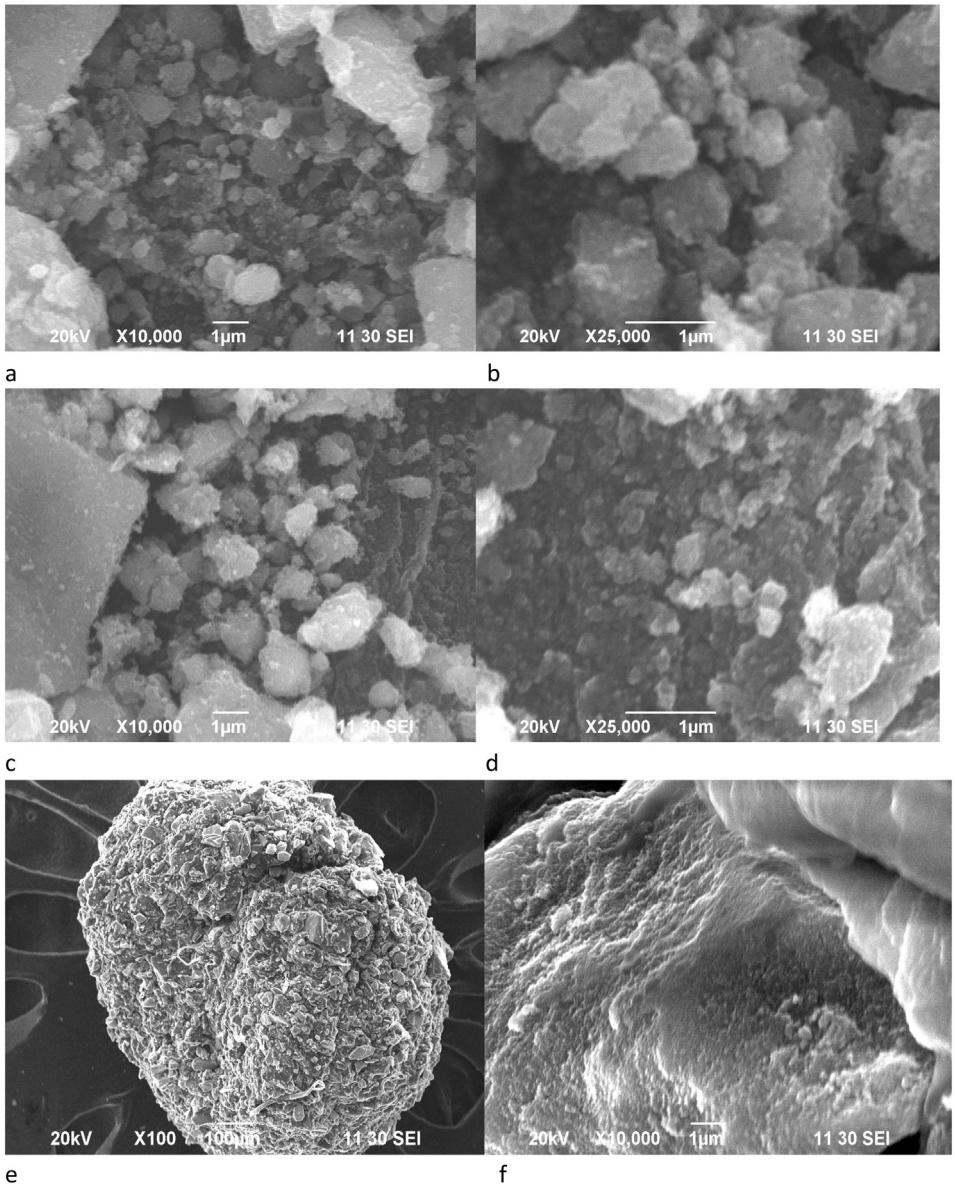

Fig. 4. SEM images of GFMNPs (a, b), GFMNPECABs powder (c, d) and the surface morphology of GFMNPECABs (e, f).

surface of GFMNPECABs powder images shown in Fig. 4c,d also showed roughness of the surface and the presence of GFMNPs on their surface. The surface morphology of GFMNPECABs shown in Fig. 4e,f indicated irregular structure with large surface area which enhanced the adsorption capacity of this adsorbent [36]. Thus, the FTIR, VSM and SEM results confirmed that the magnetic Fe_3O_4 NPs functionalized by glycine successfully entrapped into the polymer i.e. led to the formation of GFMNPECABs.

3.2. Effect of pH on Pb(II) adsorption

The effect of pH is quite significant for the adsorption mechanism and an important operational parameter for the removal of Pb(II) ions from aqueous solution. It affects the surface charge of the adsorbent as well as the concentration of adsorbate on the surface of the adsorbent [12]. The effect of pH on the % removal of Pb(II) ions was studied in the pH range 2–6. An increase in pH from 2 to 3.5 increased the removal percentage of Pb(II) ions and the maximum removal capacity of 99.7% was found after pH 4 and achieved equilibrium at pH 6 (Fig. 5). Increasing pH higher than 6 resulted in precipitation of $Pb(OH)_2$ [5]. Another limitation is that at pH below 2, the magnetic gel beads started dissolving. The carboxylate ($-COO^-$) and amino ($-NH_2$) groups are binding groups of GFMNPECABs. The alginate has carboxylate groups while GFMNPs have amino groups on GFMNPECABs' surface. At a lower pH, GFMNPs have positive charge on amino group [33] while carboxylic groups are protonated in the polymer beads [10] due to acidic conditions where presence of large number of hydrogen ions (H^+) caused protonation in the binding sites and reduced the attraction between the adsorbent and the adsorbate [37]. An increase in the pH increased the number of $-COO^-$ ions and free $-NH_2$ groups on the surface of adsorbent (GFMNPECABs) which increased the electrostatic attraction between GFMNPECABs and Pb(II) ions. Thus, the most probable adsorption mechanism of Pb(II) ions is shown in Fig. 6.

3.3. The effect of time on Pb(II) removal

Time is crucial for the evaluation of the rapidness of the adsorption process. The effect of time on the percentage removal of Pb(II) ions was evaluated up to 120 min as shown in Fig. 7. Initially the adsorption of Pb(II) ions was quite fast where 92.8% Pb(II) ions removal was achieved within just 10 min and then it became quite slow as time elapsed. The adsorption reached equilibrium with 99.7% of Pb(II) ions removed within 100 min. This is due to the fact that initially, adsorbate concentration was high and vacant active sites on the adsorbent surface were present in large numbers which caused fast as well as higher removal of Pb(II) ions. The removal rate decreased due to a significant

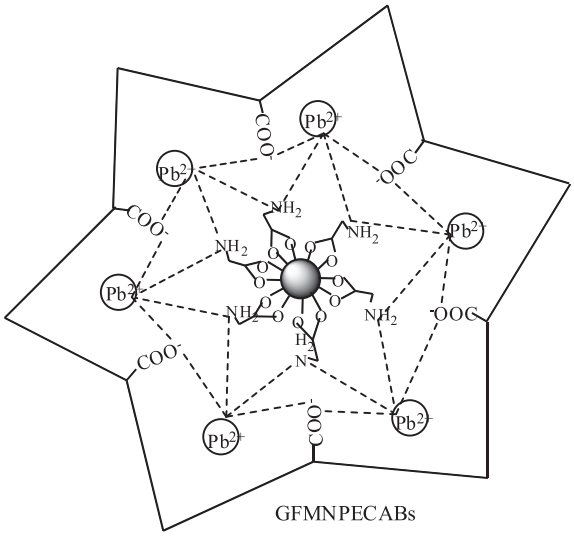

Fig. 6. The most probable adsorption mechanism of Pb(II) ions on GFMNPECABs.

decrease in the number of active sites on the adsorbent. Therefore, the removal percentage was quite fast and high (92.8%) in the first 10 min.

3.4. Adsorption isotherms

The equilibrium adsorption isotherm is quite important to describe the mechanism of the adsorption i.e. how Pb(II) ions interact with the adsorbent. It shows the relationship between the amounts of adsorbate adsorbed per unit mass of the adsorbent at a constant temperature under equilibrium conditions. For the removal of Pb(II) ions, Langmuir, Freundlich and Temkin adsorption isotherm models were used for evaluating the adsorption equilibria [38]. The results of the experimental data from the present study were fitted to these three isotherm models for elucidation of the adsorption mechanism.

The Langmuir model discusses monolayer adsorption on the homogenous surface of the adsorbent [38]. The linear form of Langmuir adsorption isotherm model is given by Eq. (4) where C_e and q_e are the equilibrium concentration and equilibrium adsorption capacity (mg/L) of Pb(II) ions, respectively, K_L is the Langmuir adsorption constant (L/mg) and Q_m is the maximum adsorption capacity at monolayer coverage (mg/g). The plot of C_e/q_e against C_e at different temperatures is shown in Fig. 8a while the corresponding calculated data is given in Table 1.

$$\frac{C_e}{q_e} = \frac{1}{K_L Q_m} + \frac{C_e}{Qm} \tag{4}$$

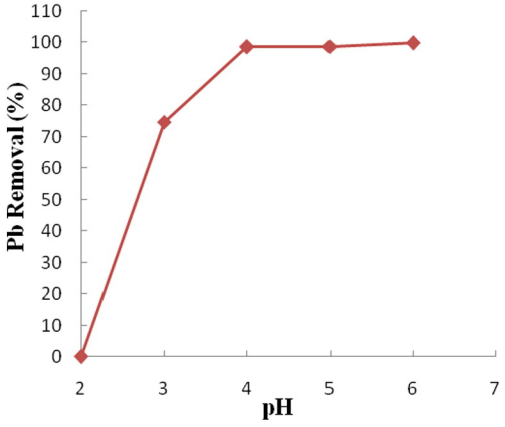

Fig. 5. Effect of pH on adsorption of Pb(II) ions by GFMNPECABs at initial concentration 10 mg/L, temperature 313 K, adsorbent dose 10 g/L and contact time 100 min.

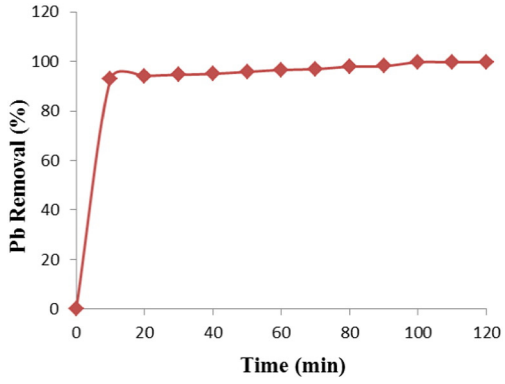

Fig. 7. The effect of time on the adsorption of Pb(II) ions by GFMNPECABs at initial concentration 10 mg/L, temperature 313 K, adsorbent dose 10 g/L and pH 6.

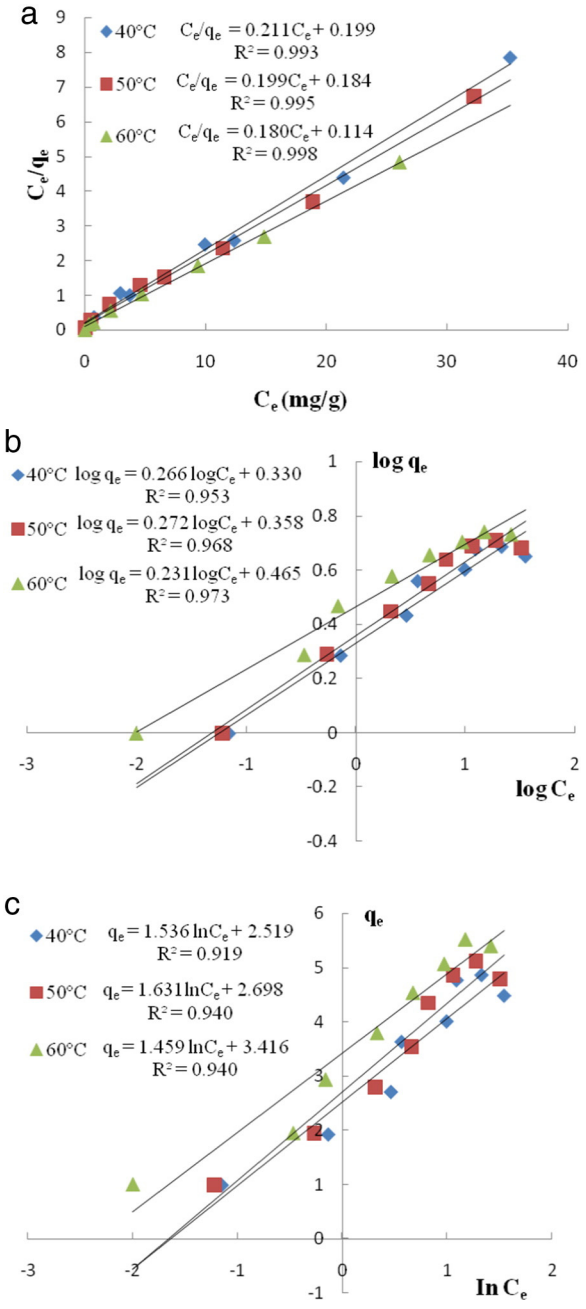

Fig. 8. Adsorption isotherm fitted to (a) Langmuir (b) Freundlich (c) Temkin models for Pb(II) ions adsorption by GFMNPECABs at initial concentration 10–80 mg/L, contact time 100 min, adsorbent dose 10 g/L and pH 6.

The dimensionless constant R_L is an essential characteristic of the Langmuir isotherm model which shows the nature of the adsorption process as unfavorable ($R_L > 1$), favorable ($0 < R_L < 1$), linear ($R_L = 1$) or irreversible ($R_L = 0$). The R_L value was calculated using Eq. (5) where C_o is the initial concentration of Pb(II) ions (mg/L).

$$R_L = \frac{1}{1 + K_L C_o} \tag{5}$$

The Freundlich model is applicable to multilayer adsorption on the heterogeneous surface of adsorbent and active sites with different energy. The linear form of the Freundlich model is given by Eq. (6) where K_F (L/mg) and n are Freundlich constants which indicate the adsorption capacity and adsorption intensity, respectively. C_e and q_e are the equilibrium concentration and equilibrium adsorption capacity (mg/L) of Pb(II) ions, respectively. The plot of log q_e against C_e at different temperatures is shown in Fig. 8b. The value of K_F and 1/n for adsorption of Pb(II) ions was obtained from the slope and the intercept of the linear plot of log q_e versus log C_e and are presented in Table 1.

Table 1
Langmuir, Freundlich, Temkin isotherm parameters for Pb(II) ions adsorption by GFMNPECABs at initial concentration 10–80 mg/L, contact time 100 min, adsorbent dose 10 g/L and pH 6.

Isotherm models and parameters	Temperature		
	40 °C	50 °C	60 °C
Langmuir			
$K_L \times 10^{-3}$(L/mg)	1.060	1.081	1.579
Q_m (mg/g)	473.9	502.5	555.5
R_L	0.086	0.084	0.059
R^2	0.993	0.995	0.998
Freundlich			
1/n	0.266	0.272	0.231
K_F (L/mg)	2.139	2.280	2.917
R^2	0.953	0.968	0.973
Temkin			
B_1	1.536	1.631	1.459
K_T (L/mg)	5.150	5.240	10.39
R^2	0.919	0.940	0.940

$$\log q_e = \log K_F + (1/n)\log C_e \tag{6}$$

The Temkin model considers the heat of adsorption of molecules which on the surface of adsorbent decreased linearly with saturation due to the adsorbate-adsorbent interaction i.e. it explains adsorbate-adsorbent interaction isotherms. The Temkin isotherm model given by Eq. (7) is simplified as in Eq. (8) where $B_1 = RT/b$, T is temperature in K, R is the universal gas constant, K_T is the equilibrium binding constant (L/mg) and B_1 is related to the heat of adsorption. C_e and q_e are the equilibrium concentration and equilibrium adsorption capacity (mg/L) of Pb(II) ions. The plots of q_e against ln C_e at the different temperatures are shown in Fig. 8c, from which the values of B_1 and K_T for the adsorption of Pb(II) ions at the different temperatures were evaluated and are presented in Table 1.

$$q_e = \frac{RT}{b} 1n(K_T C_e) \tag{7}$$

$$q_e = B_1 1n\ K_T + B_1 1n\ C_e \tag{8}$$

The results of the three isotherm parameters at different temperature are summarized in Table 1. The well fitted results at all the temperatures with high correlation coefficients ($R^2 = 0.999$) for Langmuir model suggest monolayer adsorption of Pb(II) ions on GFMNPECABs. Thus, the values of the maximum adsorption capacity, Q_m, corresponding to the Langmuir model were calculated as 473.9, 502.5 and 555.5 mg/g at 40 °C, 50 °C and 60 °C, respectively (Table 1). The Q_m increased with increasing temperature. Thus, the adsorption was favorable at higher temperature. The Langmuir isotherm characteristic constant R_L values at the different temperatures were found between 0 and 1 and thus was favorable for the adsorption of the Pb(II) ions. In Freundlich adsorption isotherm, the value of 1/n calculated was also within 0 to 1 which showed that the intensity of Pb(II) ions adsorption was favorable. However, the correlation coefficients (R^2) were lower in comparison to those obtained in the Langmuir the model (Table 1). The R^2 values in of the Temkin model were lower in comparison to the other two models which (Table 1) indicated that this model was not followed by the adsorption process. From the above results, it was concluded that chemisorptions are involved in Pb(II) ions adsorption on GFMNPECABs.

3.5. The adsorption kinetics

The adsorption kinetics is very useful for the determination of the rate-controlling step of adsorption which helps in the modeling and designing of the adsorption process. The pseudo first order and pseudo second order [39], Elovich model [38] and intraparticle diffusion models [40] were used to evaluate the kinetic data in the present study. The linearized form of the pseudo first order adsorption kinetics is expressed in Eq. (9) where q_e and q_t are the adsorption capacity (mg/g) at equilibrium and at time t (min), respectively and k_1 is the rate constant (min^{-1}) for the pseudo first order adsorption model. This model is based on the assumption of physical adsorption. The plots of log (q_e-q_t) against t at different temperatures (40, 50 and 60 °C) are shown in Fig. 9a. The values of the rate constants k_1 were calculated from the slopes of the plots of log (q_e-q_t) versus t and are presented in Table 2.

$$\log(q_e - q_t) = \log q_e - \frac{k_1}{2.303}t \quad (9)$$

The linearized pseudo second order adsorption kinetic model which is based on chemisorptions is given by Eq. (10) where k_2 (g mg^{-1} min^{-1}) is the pseudo second order rate constant. The plots of t/q_t against time t at different temperatures are shown in Fig. 9b which show excellent linearity. The values of k_2 were calculated from the intercept of the linear plots of t/q_t versus t and are given in Table 2.

$$\frac{t}{q_t} = \frac{1}{k_2 q_e^{\,2}} + \frac{1}{q_e}t \quad (10)$$

The Elovich model has satisfactorily been applied for chemisorption process whereby the surface of adsorbent is covered at a slow adsorption rate and is often valid for heterogeneous surface of the adsorbent [41]. It is expressed in the linear form as shown in Eq. (11) where q_t is the amount of the metal ions adsorbed on adsorbents (mg/g) at time t (min) while a (mg/g) and b (mg/g) are the Elovich constants. The values of a and b (Table 2) were calculated from slopes and intercepts, respectively, of the plots of q_t versus ln t at different temperatures as shown in Fig. 9c.

$$q_t = a + b\ \ln\ t \quad (11)$$

Table 2
Kinetic parameters for Pb(II) adsorption by GFMNPECABs at initial concentration 10 mg/L, contact time 100 min, adsorbent dose 10 g/L and pH 6.

Kinetic models and parameters	Temperature		
	40 °C	50 °C	60 °C
Pseudo first order			
k_1 (min^{-1})	0.034	0.032	0.016
R^2	0.939	0.804	0.963
Pseudo second order			
k_2 (g mg^{-1} min^{-1})	0.266	0.769	0.613
R^2	0.999	0.999	0.999
Elovich model			
a (mg/g^{-1})	0.384	0.864	0.859
b (mg/g^{-1})	0.132	0.024	0.026
R^2	0.886	0.942	0.890
Intraparticle diffusion			
A (mg^{-1} g)	0.603	0.899	0.897
k_{id} (mg/g^{-1} min^{-1})	0.040	0.008	0.009
R^2	0.769	0.985	0.958

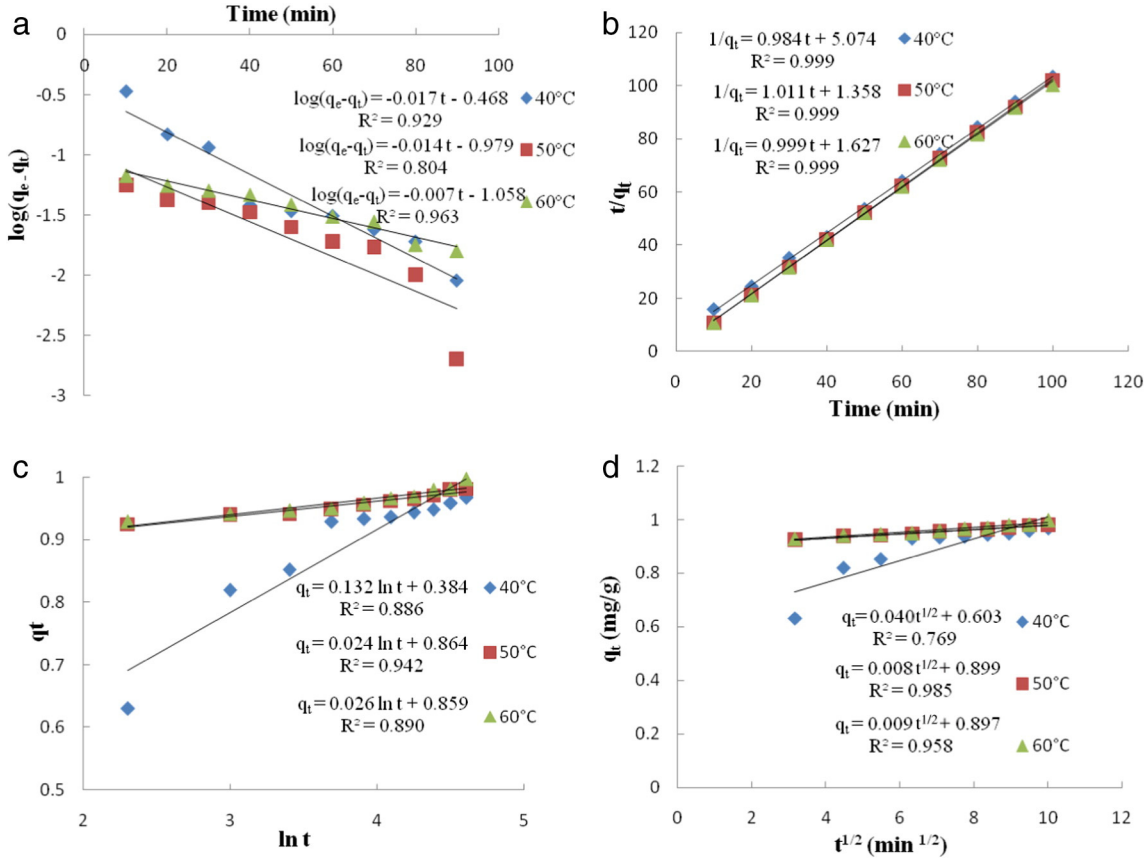

Fig. 9. Kinetic models for (a) pseudo first order (b) pseudo second order (c) Elovich (d) intraparticle diffusion adsorption of Pb(II) ions by GFMNPECABs at initial concentration 10–80 mg/L, contact time 100 min, adsorbent dose 10 g/L and pH 6.

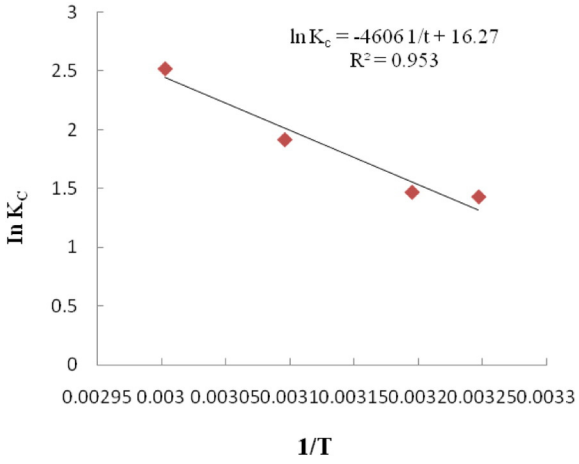

Fig. 10. Van't Hoff's plot for removal of Pb(II) ions by GFMNPECABs.

The intraparticle diffusion model considers adsorption as a multiple process [40]. It is due to the fact that the adsorbate is adsorbed on the surface of the adsorbent followed by their diffusion into the interior pores of the adsorbents. The linear form of the interparticle diffusion model is given by Eq. (12) where q_t is the adsorption capacity (mg/g) at t time (min), k_{id} is the diffusion rate constant (mg/g $min^{½}$) and A (mg/g) is a constant. The plots q_t against $t^{1/2}$ at 40, 50 and 60 °C are shown in Fig. 9d from which the values of k_{id} and A were obtained as presented in Table 2.

$$q_t = K_{id}\sqrt{t} + A \tag{12}$$

The kinetic parameters for the different kinetic models obtained at the different temperatures are summarized in Table 2. The values of correlation coefficient (R^2) of pseudo second order adsorption were very close to unity ($R^2 = 0.999$) at three temperatures, and much higher than those found in other models. It confirmed that the adsorption of the Pb(II) ions followed the chemisorptions mechanism which was further supported by the adsorption isotherm analysis (cf. Section 3.4). The correlation coefficients as in the case of the pseudo first order and intraparticle diffusion models were near to unity but not as higher as in the case of the second order kinetic model. The Elovich model showed correlation coefficient value the lowest among all the kinetic models studied in the present case. Therefore, it was concluded that some weak interactions and intraparticle diffusion are involved in the adsorption process [42].

3.6. Thermodynamic studies

The thermodynamic parameters were evaluated to further confirm the nature of the adsorption process. The Gibbs free energy change (ΔG°), enthalpy change (ΔE°) and entropy change (ΔS°) provide information about feasibility and spontaneous nature of the adsorption process. The thermodynamic equilibrium constant (K_c) [1] and Gibbs free energy change (ΔG°) were calculated using Eqs. (13) and (14), respectively where C_A and C_B are the Pb(II) ions concentration on the adsorbent and the residual equilibrium concentration [43]. The value of enthalpy change (ΔH°) and entropy change (ΔS°) were calculated from the Van't Hoff Eq. (15) [1].

$$K_c = \frac{C_A}{C_B} \tag{13}$$

$$\Delta G^\circ = -RT1nK_c \tag{14}$$

$$1n\ K_c = \frac{\Delta S^\circ}{R} - \frac{\Delta H^\circ}{RT} \tag{15}$$

The plot of ln K_c against 1/T (Fig. 10) was used to evaluate ΔS°. The calculated values of the thermodynamic parameters viz. ΔG° were −3.655, −3.817, −5.1440 and −6.981 kJ mol^{-1} at 308, 313, 323 and 333 K, respectively while ΔH° and ΔS° were found to be 38.294 kJ mol^{-1} and ΔS° 135.26 J mol^{-1} K, respectively. The negative values of ΔG° indicate spontaneity and feasibility of the Pb(II) ions removal process while the positive value of ΔH° indicates the endothermic nature of the chemisorption process. The positive value of ΔS° indicates the randomness at the solid-liquid interface during the adsorption of Pb(II) ions.

3.7. Comparison with other adsorbents

A comparison with other adsorbents reported in literature on the basis of the optimum pH; fitted adsorption isotherms, kinetics, contact time and the adsorption capacity is presented in Table 3. The results indicate that the adsorption capacity of the present synthesized

Table 3
Comparison of adsorption capacity of various adsorbents for the removal of Pb(II) ions.

Type of adsorbent used	Optimum pH; fitted adsorption isotherms; kinetics; contact time; comments	Adsorption capacity, Q_m (mg/g)	Ref.
Magnetic alginate beads based on maghemite nanoparticles	95.2% of the Pb(II) removed within 2 h at pH 7, followed Langmuir adsorption equation, regenerated sorbent in repeated sorption-desorption cycles.	50.00	44
Calcium alginate xerogels and immobilized *Fucus vesiculosus*	Intraparticle diffusion, calcium in the gels was displaced by Pb from solution according to the "egg-box" model.	58.02	45
Polyaniline nanofibers assembled on alginate microsphere	Batch adsorption at pH range 3–7, adsorption reached equilibrium within 40 min, followed pseudo-second-order kinetics, desorption was 75%.	251.40	46
Three adsorbents; Chitosan and chitosan derivatives beads	pH 5, adsorption capacities for Langmuir isotherm for chitosan, chitosan-GLA and chitosan-alginate beads 34.98, 14.24 and 60.27 mg/g, respectively.	60.27 chitosan-alginate beads	47
Chitosan/Fe_3O_4 nanocomposite beads	Maximum adsorption capacity at pH 6, a promising adsorbent not only for Pb(II) and Ni(II) in pH = 4–6 but many metals.	63.33	48
Entrapped silica nanopowders within calcium alginate beads	pH 5, equilibrium reached in 90 min, followed Langmuir isotherm and pseudo-second order kinetics.	83.33	49
Polyaniline grafted cross-linked chitosan beads	pH 5, the maximum adsorption capacity at 45 °C, followed Langmuir model and pseudo-second-order kinetic model. 0.5 M HCl desorbed the spent adsorbent 97.50% in 3 h.	114.00	50
Mesoporous silica-grafted graphene oxide	The maximum adsorption achieved within 10 min over pH range 4–7, selectively adsorb >99% of Pb(II).	255.10	51
GFMNPECABs	pH 6, 92.8% Pb(II) was removed in 10 min, equilibrium 100 min with 99.8% Pb(II) removal, followed Langmuir isotherm and pseudo second order model, regenerated 4 times by 0.2 M HNO_3, with 90% adsorption capacity; eco-friendly, cost effective, efficient and superior over polymer based adsorbents.	555.50	Present work

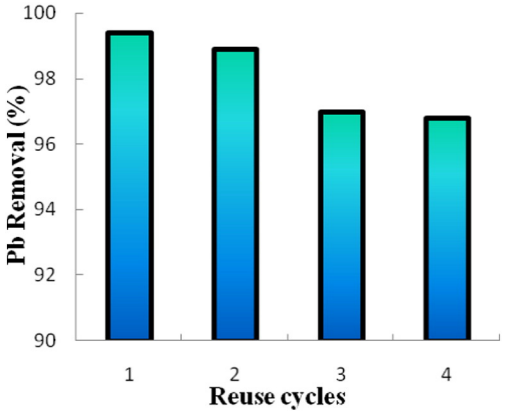

Fig. 11. Relationship between reuse cycles and the percentage removal of Pb(II) ions by GFMNPECABs at initial concentration 10 mg/L, temperature 313 K, adsorbent dose 10 g/L and pH 6.

adsorbent is higher than any other adsorbents reported [44–51]. The GFMNPECABs show maximum adsorption capacity 555.5 mg/g due to higher affinity of amino and carboxylate groups present on the surface of the adsorbents i.e. GFMNPECABs.

3.8. Desorption and reusability study

The regeneration of the adsorbent is an important feature for economic feasibility and determination of stability of the adsorbent. In the present study, regeneration of the adsorbent was attempted by 0.2 M HNO_3 acid where the adsorbent was shaken at 30 °C for 30 min and reused. The adsorption showed four times the regeneration cycles maintaining >90% of adsorption capacity (Fig. 11). Thus, due to the high recycling potential of GFMNPECABs, it can be reused as an effective adsorbent for the removal of Pb(II) ions from aqueous solution without significant loss of their initial adsorption capacity.

4. Conclusion

The present study confirmed that the glycine-functionalized magnetic NPs entrapped calcium alginate beads were quite effective for Pb(II) ions removal from aqueous solution. The proposed method provides a cost-effective and eco-friendly means for the removal of Pb(II) ions from water samples. The Pb(II) uptake reached equilibrium only in 100 min and efficiently removed Pb(II) ions up to 99.8%. The maximum adsorption capacity was found to be 555.5 mg/g at pH 6. The equilibrium data fitted well in Langmuir and Freundlich models. The kinetic data follows pseudo second order kinetic model. Based on the thermodynamic parameters, the adsorption process was confirmed as endothermic in nature. The adsorbent could be regenerated four times retaining 90% adsorption capacity. The GFMNPECABs were easily separated by external magnetic field which suggested that this method is clean, convenient and safe for water treatment meeting the requirements of green chemistry.

Acknowledgement

A. Asthana is thankful to the University Grants Commission Regional Office, Bhopal, Madhya Pradesh, India, for sanction of a minor research project grant. S. Prasad is grateful to the University of the South Pacific, Suva, Fiji for support in various ways.

References

[1] J. Feng, Z. Yang, G. Zeng, J. Huang, H. Xu, Y. Zhang, S. Wei, L. Wang, The adsorption behavior and mechanism investigation of Pb(II) removal by flocculation using microbial flocculant GA1, Bioresour. Technol. 148 (2013) 414–421.
[2] C.-G. Lee, J.-W. Jeon, M.-J. Hwang, K.-H. Ahn, C. Park, J.-W. Choi, S.-H. Lee, Lead and copper removal from aqueous solutions using carbon foam derived from phenol resin, Chemosphere 130 (2015) 59–65.
[3] A. Masoumi, K. Hemmati, M. Ghaemy, Low-cost nanoparticles sorbent from modified rice husk and a copolymer for efficient removal of Pb(II) and crystal violet from water, Chemosphere 146 (2016) 253–262.
[4] J.P. Maity, Y.M. Huang, C.-M. Hsu, C.-I. Wu, C.-C. Chen, C.-Y. Li, J.-S. Jean, Y.-F. Chang, C.-Y. Chen, Removal of Cu, Pb and Zn by foam fractionation and a soil washing process from contaminated industrial soils using soapberry-derived saponin: a comparative effectiveness assessment, Chemosphere 92 (2013) 1286–1293.
[5] B. Liu, X. Lv, X. Meng, G. Yu, D. Wang, Removal of Pb(II) from aqueous solution using dithiocarbamate modified chitosan beads with Pb(II) as imprinted ions, Chem. Eng. J. 220 (2013) 412–419.
[6] X. Peng, F. Xu, W. Zhang, J. Wang, C. Zeng, M. Niu, E. Chmielewska, Magnetic Fe_3O_4 silica xanthan gum composites for aqueous removal and recovery of Pb^{2+}, Colloids Surf. A Physicochem. Eng. Asp. 443 (2014) 27–36.
[7] X.W. Peng, L.X. Zhong, J.L. Ren, R.C. Sun, Highly effective adsorption of heavy metal ions from aqueous solutions by macroporous xylan-rich hemicelluloses-based hydrogel, J. Agric. Food Chem. 60 (2012) 3909–3916.
[8] P. Xu, G.M. Zeng, D.L. Huang, C.L. Feng, S. Hu, M.H. Zhao, C. Lai, Z. Wei, C. Huang, G.X. Xie, Z.F. Liu, Use of iron oxide nanomaterials in wastewater treatment: A review, Sci. Total Environ. 424 (2012) 1–10.
[9] X. Zhao, L. Lv, B. Pan, W. Zhang, S. Zhang, Q. Zhang, Polymer-supported nanocomposites for environmental application: A review, Chem. Eng. J. 170 (2011) 381–394.
[10] V. Rocher, J.M. Siaugue, V. Cabuil, A. Bee, Removal of organic dyes by magnetic alginate beads, Water Res. 42 (2008) 1290–1298.
[11] A.F. Ngomsika, A. Beea, J.M. Siauguea, V. Cabuila, G. Coteb, Nickel adsorption by magnetic alginate microcapsules containing an extractant, Water Res. 40 (2006) 1848–1856.
[12] Y.T. Zhou, H.L. Nie, C.B. White, Z.Y. He, L.M. Zhu, Removal of Cu^{2+} from aqueous solution by chitosan-coated magnetic nanoparticles modified with α-ketoglutaric acid, J. Colloid Interface Sci. 330 (2009) 29–37.
[13] H. Yan, L. Yang, Z. Yang, H. Yang, A. Li, R. Cheng, Preparation of chitosan/poly(acrylic acid) magnetic composite microspheres and applications in the removal of copper(II) ions from aqueous solutions, J. Hazard. Mater. 229–230 (2012) 371–380.
[14] D. Wu, J. Zhao, L. Zhang, Q. Wu, Y. Yang, Lanthanum adsorption using iron oxide loaded calcium alginate beads, Hydrometallurgy 101 (2010) 76–83.
[15] A.B.D. Talbot, S. Abramson, V. Dupuis, Magnetic alginate beads for Pb(II) ions removal from wastewater, J. Colloid Interface Sci. 362 (2011) 486–492.
[16] S.H. Huang, D.H. Chen, Rapid removal of heavy metal cations and anions from aqueous solutions by an amino-functionalized magnetic nano-adsorbent, J. Hazard. Mater. 163 (2009) 174–179.
[17] I.Y. Goon, C.C. Zhang, M. Lim, J.J. Gooding, R. Amal, Controlled fabrication of polyethylenimine-functionalized magnetic nanoparticles for the sequestration and quantification of free Cu^{2+}, Langmuir 26 (2010) 12247–12252.
[18] H. Ebrahimzadeh, A.A. Asgharinezhad, E. Moazzen, M.M. Amini, O. Sadeghi, A magnetic ion-imprinted polymer for lead(II) determination: A study on the adsorption of lead(II) by beverages, J. Food Compos. Anal. 41 (2015) 74–80.
[19] Y. Zhou, S. Fu, L. Zhang, H. Zhan, M.V. Levit, Use of carboxylated cellulose nanofibrils-filled magnetic chitosan hydrogel beads as adsorbents for Pb(II), Carbohydr. Polym. 101 (2014) 75–82.
[20] E.N. Zare, M.M. Lakouraj, A. Ramezani, Efficient sorption of Pb(II) from an aqueous solution using a poly(aniline-*co*-3-aminobenzoic acid)-based magnetic core–shell nanocomposite, New J. Chem. 40 (2016) 2521–2529.
[21] H.E. Khal, N.H. Batis, Effects of temperature on the preparation and characteristics of hydroxyapatite and its adsorptive properties toward lead, New J. Chem. 39 (2015) 3597–3607.
[22] S. Thatai, P. Khurana, S. Prasad, S.K. Soni, D. Kumar, Trace colorimetric detection of Pb^{2+} using plasmonic gold nanoparticles and silica-gold nanocomposites, Microchem. J. 124 (2016) 104–110.
[23] R.M. Naik, B. Kumar, S. Prasad, A.A. Chetty, A. Asthana, Catalytic ligand exchange reaction between hexacyanoferrate(II) and 4-cyanopyridine applied to trace kinetic analysis of palladium(II), Microchem. J. 122 (2015) 82–88.
[24] J. Boken, S. Thatai, P. Khurana, S. Prasad, D. Kumar, Highly selective visual monitoring of hazardous fluoride ion in aqueous media using thiobarbituric-capped gold nanoparticles, Talanta 132 (2015) 278–284.
[25] S. Thatai, P. Khurana, S. Prasad, D. Kumar, Plasmonic detection of Cd^{2+} ions using surface-enhanced raman scattering active core-shell nanocomposite, Talanta 134 (2015) 568–575.
[26] G.P. Pandey, A.K. Singh, S. Prasad, L. Deshmukh, A. Asthana, Development of surfactant assisted kinetic method for trace determination of thallium in environmental samples, Microchem. J. 118 (2015) 150–157 (and references cited therein).
[27] V. Chand, S. Prasad, Trace determination and chemical speciation of selenium in environmental water samples using catalytic kinetic spectrophotometric method, J. Hazard. Mater. 165 (2009) 780–788.
[28] R. Prasad, R. Kumar, S. Prasad, A fluorescence quenching-based sensor using new metallo-tetraazaporphyrin dye as a recognition element for aniline assay in aqueous solutions, Anal. Chim. Acta 646 (2009) 97–103.
[29] V. Tomar, S. Prasad, D. Kumar, Adsorptive removal of fluoride from water samples using Zr-Mn composite material, Microchem. J. 111 (2013) 116–124 (and references cited therein).
[30] V. Tomar, S. Prasad, D. Kumar, Adsorption study on removal of fluoride in aqueous media using *Citrus limonum*, Microchem. J. 112 (2014) 97–103 (and references cited therein).
[31] V. Chaudhary, S. Prasad, Rapid removal of fluoride from aqueous media using activated dolomite, Anal. Methods 7 (2015) 8304–8314.

[32] L. Zhou, Y. Wang, Z. Liu, Q. Huang, Characteristics of equilibrium, kinetics studies for adsorption of Hg(II), Cu(II), and Ni(II) ions by thiourea-modified magnetic chitosan microspheres, J. Hazard. Mater. 161 (2009) 995–1002.
[33] N.C. Feitoza, T.D. Goncalves, J.J. Mesquita, J.S. Menegucci, M.K.M.S. Santos, J.A. Chaker, R.B. Cunha, A.M.M. Medeiros, J.C. Rubim, M.H. Sousa, Fabrication of glycine-functionalized maghemite nanoparticles for magnetic removal of copper from wastewater, J. Hazard. Mater. 264 (2014) 153–160.
[34] J. Wang, K. Pan, Q. He, B. Cao, Polyacrylonitrile/polypyrrole core/shell nanofiber mat for the removal of hexavalent chromium from aqueous solution, J. Hazard. Mater. 244–245 (2013) 121–129.
[35] K.C. Barick, P.A. Hassan, Glycine passivated Fe_3O_4 nanoparticles for thermal therapy, J. Colloid Interface Sci. 369 (2012) 96–102.
[36] V. Gopalakannan, N. Viswanathan, Synthesis of magnetic alginate hybrid beads for efficient chromium(VI), Int. J. Biol. Macromol. 72 (2015) 862–867.
[37] W.S. Tan, A.S.Y. Ting, Alginate-immobilized bentonite clay: Adsorption efficacy and reusability for Cu(II) removal from aqueous solution, Bioresour. Technol. 160 (2014) 115–118.
[38] N.K. Amin, Removal of direct blue-106 dye from aqueous solution using new activated carbons developed from pomegranate peel: Adsorption equilibrium and kinetics, J. Hazard. Mater. 165 (2009) 52–62.
[39] A.E. Nemr, Potential of pomegranate husk carbon for Cr(VI) removal from wastewater: Kinetic and isotherm studies, J. Hazard. Mater. 161 (2009) 132–141.
[40] F.C. Wu, R.L. Tseng, R.S. Juang, Initial behavior of intraparticle diffusion model used in the description of adsorption kinetics, Chem. Eng. J. 153 (2009) 1–8.
[41] M.R. Lasheen, N.S. Ammar, H.S. Ibrahim, Adsorption/desorption of Cd(II), Cu(II) and Pb(II) using chemically modified orange peel: Equilibrium and kinetic studies, Solid State Sci. 14 (2012) 202–210.
[42] J. Dai, H. Yan, H. Yang, R. Cheng, Simple method for preparation of chitosan/poly(acrylic acid) blending hydrogel beads and adsorption of copper(II) from aqueous solutions, Chem. Eng. J. 165 (2010) 240–249.
[43] V.M. Boddu, K. Abburi, J.L. Talbott, E.D. Smith, R. Haasch, Removal of arsenic(III) and arsenic(V) from aqueous medium using chitosan coated biosorbent, Water Res. 42 (2008) 633–642.
[44] A. Idris, N.S.M. Ismail, N. Hassan, E. Misran, A.F. Ngomsik, Synthesis of magnetic alginate beads based on maghemite nanoparticles for Pb(II) removal in aqueous solution, J. Ind. Eng. Chem. 18 (2012) 1582–1589.
[45] Y.N. Mata, M.L. Blazquez, A. Ballester, F. Gonzalez, J.A. Munoz, Biosorption of cadmium, lead and copper with calcium alginate xerogels and immobilized *Fucus vesiculosus*, J. Hazard. Mater. 163 (2009) 555–562.
[46] N. Jiang, Y. Xu, Y. Dai, W. Luo, L. Dai, Polyaniline nanofibers assembled on alginate microsphere for Cu^{2+} and Pb^{2+} uptake, J. Hazard. Mater. 215–216 (2012) 17–24.
[47] W.S.W. Ngah, S. Fatinathan, Pb(II) biosorption using chitosan and chitosan derivatives beads: equilibrium, ion exchange and mechanism studies, J. Environ. Sci. 22 (2010) 338–346.
[48] H.V. Tran, L.D. Tran, T.N. Nguyen, Preparation of chitosan/magnetite composite beads and their application for removal of Pb(II) and Ni(II) from aqueous solution, Mater. Sci. Eng. C 30 (2010) 304–310.
[49] R.D.C. Soltani, G.S. Khorramabadi, A.R. Khataee, S. Jorfi, Silica nanopowders/alginate composite for adsorption of lead(II) ions in aqueous solutions, J. Taiwan Inst. Chem. Eng. 45 (2014) 973–980.
[50] E. Igberase, P. Osifo, Equilibrium, kinetic, thermodynamic and desorption studies of cadmium and lead by polyaniline grafted cross-linked chitosan beads from aqueous solution, J. Ind. Eng. Chem. 26 (2015) 340–347.
[51] X. Li, Z. Wang, Q. Li, J. Ma, M. Zhu, Preparation, characterization, and application of mesoporous silica-grafted graphene oxide for highly selective lead adsorption, Chem. Eng. J. 273 (2015) 630–637.